Numerical Investigation of the Quench Behavior of $Bi_2Sr_2CaCu_2O_x$ Wire

D. Arbelaez, S. O. Prestemon, D. R. Dietderich, and A. Godeke

Lawrence Berkeley National Laboratory, 1 Cyclotron Road, Berkeley CA 94720

L. Ye, F. Hunte and J. Schwartz

Department of Materials Science and Engineering, North Carolina State University, Raleigh, NC 27695

This work was supported by the Director, Office of Energy Research, Office of High Energy and Nuclear Physics, High Energy Physics Division, U.S. Department of Energy under Contract No. DE-AC02-05CH11231.

Numerical Investigation of the Quench Behavior of $Bi_2Sr_2CaCu_2O_x$ Wire

D. Arbelaez, S. O. Prestemon, D. R. Dietderich, A. Godeke, L. Ye, F. Hunte, and J. Schwartz

***Abstract*—The quench behavior of $Bi_2Sr_2CaCu_2O_x$ (Bi2212) wire is investigated through numerical simulations. This work is part of the U.S. Very High Field Superconducting Magnet Collaboration (VHFSMC). Numerical simulations are carried out using a one-dimensional computational model of thermal transport in Bi2212 composite wires. A quench is simulated by introducing heat in a section of the wire, and the voltage and temperature are monitored as function of time and position. The quench energy, normal zone propagation velocity, and spatial distribution of temperature are calculated for varying transport current and applied magnetic field. The relevance of these simulations in defining criteria for experimental measurements is discussed.**

***Index Terms*—High temperature superconductor, quench, simulation.**

I. Introduction

In order to move beyond the intrinsic limitations of Nb based conductors for magnet technology new materials and methods must be developed. The U.S. Very High Field Superconducting Magnet Collaboration (VHFSMC) is working on the development of the necessary technology to allow the practical application of $Bi_2Sr_2CaCu_2O_x$ (Bi2212) conductors in high field magnets. Bi2212 is an attractive alternative to Nb based conductors since it has a high critical magnetic field and it is commercially available in round wire. At Lawrence Berkeley National Laboratory (LBNL) wind-and-react subscale Bi2212 coils have been constructed and tested [1]. One of the critical issues in the development of this technology is the stability of these conductors and its affect on magnet protection. Understanding the quench behavior of the Bi2212 conductors is critical for the practical application of this material in high field magnets.

At LBNL computational simulation tools are being developed to model quench propagation Bi2212 conductors. The initial focus in this project is to develop simple and efficient tools that allow for accurate modeling and parametric studies. While these models are simple, they are expected to provide information that can be used to determine where further model refinement may be needed through parametric studies. These studies can be critical in determining where effort should be placed in obtaining experimental data that can be used for predictive modeling.

Manuscript received August 03, 2010; accepted October 11, 2010. Date of publication December 30, 2010; date of current version May 27, 2011. This work was partly supported by the Director, Office of Science, High Energy Physics, US Department of Energy, under Contract DE-AC02-05CH11231, and also benefited from the American Recovery and Reinvestment Act Funding.

D. Arbelaez, S. O. Prestemon, D. R. Dietderich, and A. Godeke are with the Lawrence Berkeley National Laboratory, Berkeley, CA 94720 USA (e-mail: darbelaez@lbl.gov).

L. Ye, F. Hunte, and J. Schwartz are with the Department of Materials Science and Engineering, North Carolina State University, Raleigh, NC 27695 USA.

II. One-Dimensional Quench Model

For this model, a single partial differential equation (PDE) is solved with effective material properties defined over a cross-section. The one-dimensional heat transfer model is given by

$$\gamma C_p(T)\frac{\partial T}{\partial t} = \frac{\partial}{\partial x}\left(\kappa(T)\frac{\partial T}{\partial x}\right) + \rho(T)J_n^2 + Q, \qquad (1)$$

where $T(x,t)$ is the spatially and temporally dependent temperature, t and x are the time and space coordinates, γ is the density, C_p is the specific heat capacity, κ is the thermal conductivity, ρ is the electrical resistivity, J_n is the non-superconducting current density, Q is the external rate of heat per unit volume introduced into the system. The term Q includes the heat introduced for a quench trigger and the heat dissipated to the environment (e.g. heat lost to a liquid Helium bath). For this model, the properties shown in equation (1) are a function of the material properties for the individual phases. To simplify the notation, the index 1 will be used for Ag and the index 2 will be used for Bi2212. The homogenized value of γC_p, which is assumed to be a weighted average over the individual phases, can be written as

$$\gamma C_p = v_1\gamma_1 C_{p1} + v_2\gamma_2 C_{p2}, \qquad (2)$$

where v_1 and v_2 are the volume fractions of phase 1 (Ag) and phase 2 (Bi2212). This choice is made since the heat capacities of Ag and Bi2212 are comparable; therefore, neither one can be neglected. For the effective thermal conductivity, all of the heat conduction is assumed to take place only in the Ag phase, since the conductivity of Ag is substantially higher than that of Bi2212. Therefore, the homogenized conductivity is

$$\kappa = v_1\kappa_1, \qquad (3)$$

where the volume fraction of Ag is used to scale the effective thermal conductivity for a cross-section. The effective resistivity is given by

$$\rho = \frac{\rho_1\rho_2}{v_1\rho_2 + v_2\rho_1}, \qquad (4)$$

where this equation holds only once the Bi2212 phase becomes normal conducting. When the Bi2212 phase is superconducting, the effective resistivity is given by $\rho = \rho_1/v_1$.

The engineering current density J_e (i.e. the current density over the entire wire cross-section) is given in terms of the individual current densities as

$$J_e = \frac{I}{A_{tot}} = v_1 J_1 + v_2 J_2, \tag{5}$$

where I is the total current over the cross-section and A_{tot} is the cross-sectional area, and it is assumed that J_1 and J_2 are constant over their respective phases. For the current sharing model, it is assumed that if the current density in the Bi2212 phase is less than the critical current density for a given field and temperature, then the superconductor carries all of the current. If the current density in Bi2212 is greater than the critical current density for the given field and temperature, then the remaining current above $J_c(H,T)$ is distributed to the Ag phase and to the Bi2212 phase after the superconductor becomes a normal conductor. Therefore, the non-superconducting current density in equation (1), J_n, is equivalent to J_1. In summary, the current sharing model is

$$\begin{array}{lll} J_1 = 0 & J_2 = \frac{1}{v_2} J_e & \text{if } J_e \le v_2 J_c(H,T) \\ J_1 = \frac{J_e - v_2 J_c(H,T)}{v_1} & J_2 = J_c(H,T) & \text{if } J_e > v_2 J_c(H,T). \end{array} \tag{6}$$

III. Numerical Solution

Equation (1) is solved numerically by discretizing in both space and time. The spatial discretization is achieved by using a finite difference approach. The first term on the right hand side of equation (1) is approximated by the discrete operator $D_i[T,\kappa;\Delta x]$, which is defined here as

$$\frac{\partial}{\partial x}\left(\kappa(T)\frac{\partial T}{\partial x}\right) \approx D_i[T,\kappa;\Delta x] = \kappa_{i+1}\frac{3T_{i+1} - 4T_i + T_{i-1}}{4\Delta x^2} + \kappa_{i-1}\frac{3T_{i-1} - 4T_i + T_{i+1}}{4\Delta x^2}, \tag{7}$$

where Δx is the length of one discrete segment and T_i, T_{i+1}, and T_{i-1} correspond to the temperature at locations x, $x + \Delta x$, and $x - \Delta x$ respectively. The thermal conductivity values κ_{i+1} and κ_{i-1} correspond to $\kappa(T_{i+1})$ and $\kappa(T_{i-1})$ respectively. Using equation (7), the semi-discrete form of equation (1) is given by

$$\gamma C_{p,i} \left.\frac{\partial T}{\partial t}\right|_i = D_i[T,\kappa;\Delta x] + \rho_i J^2 + Q_i, \tag{8}$$

where the same conventions are used for the subscript i as in equation (7). The semi-discrete equation is solved using the Runge-Kutta-Fehlberg method (RKF45) which is a fourth order accurate method that uses a fifth order accurate solution to construct an error estimate. Since RKF45 is an explicit method, it can be prone to instability when the time step size is not small enough. However, the error estimate can be used for time step adaptivity such that the error at every step is maintained below a user specified tolerance. This not only provides an estimate for the error in the solution, but also ensures that small enough time steps are used to avoid instabilities.

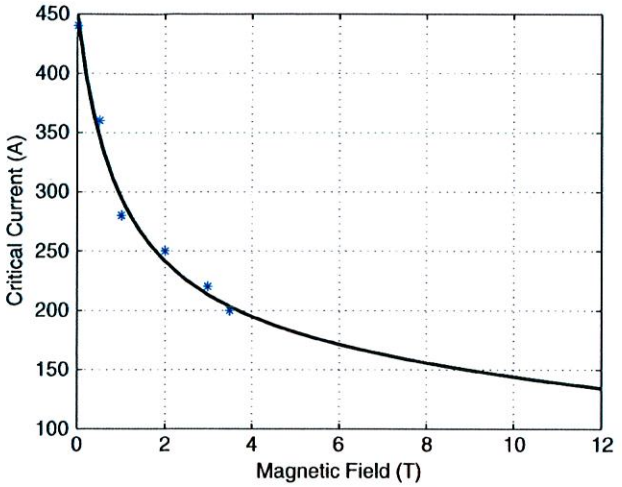

Fig. 1. (Asterisk) Measured critical current of Bi2212 wires in liquid He and (solid line) the model given in equation (9) with parameters chosen to fit the experimental data.

Initial and boundary conditions must be specified for the solution of equation (8). For the simulations considered in this paper, the initial condition is always set to be a constant temperature of 4.2 K over the entire domain. The boundary conditions are chosen to satisfy an adiabatic assumption at the ends of the wire. Therefore, $\partial T/\partial x$ is forced to vanish at the boundaries. Due to the symmetry of the problem, only half of the domain needs to be modeled with $\partial T/\partial x$ forced to vanish at the peak of the hot spot. For the remainder of the paper it will be assumed without loss of generality that the symmetry point occurs at $x = 0$ (i.e. the hot spot location is $x = 0$).

IV. Critical Current Density

The quality of the simulation is highly dependent on the material behavior input. An accurate description of the temperature and magnetic field dependence of critical current density is essential for capturing the correct quench behavior. A model that is used in [2] and [3] to study current instabilities in Bi based conductors and was introduced in [4] is used to fit the critical surface of the Bi2212 conductor. The model is given by

$$J_c(T,B) = J_0\left(1 - \frac{T}{T_c}\right)^{\gamma}\left[(1-\chi)\frac{B_0}{B_0 + B} + \chi \exp\left(-\frac{\beta B}{(B_{c,0}\exp(-\alpha T/T_c)}\right)\right], \tag{9}$$

where the following quantities are used: $T_c = 87.1$ K, $B_{c,0} = 465.5$ T, $\alpha = 10.33$, $\beta = 6.76$, $\gamma = 1.73$, $J_0 = 1600.0$ A/mm^2, $B_0 = 1.0$ T, and $\chi = 0.33$. The quantities J_0, and χ were chosen to best fit experimental data that was obtained on Bi2212 wires for applied magnetic field between 0 and 3.5 T at 4.2 K [5]. The remaining parameters were taken to be those given in [2]. Fig. 1 shows the experimental values of critical current along with the best fit model given by equation (9). Clearly more data is needed at higher applied magnetic field to assess the accuracy of the fit; however, for the limited range the model is able to fit the data accurately. Fig. 2 shows the critical surface for the Bi2212 conductor for

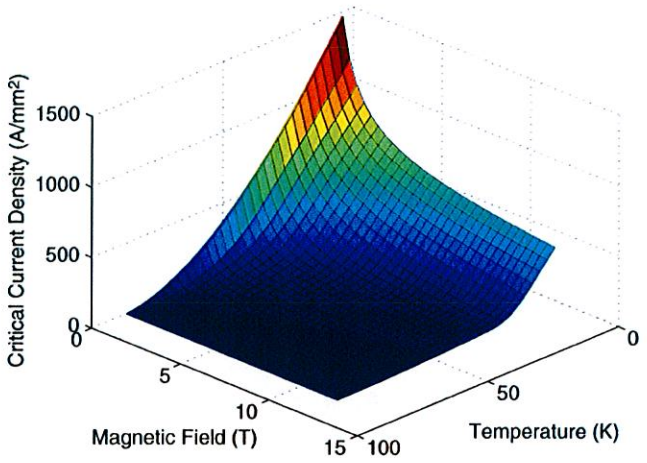

Fig. 2. Critical current density as a function of temperature and applied magnetic field as given by equation (9) and fit to the data from Fig. 1.

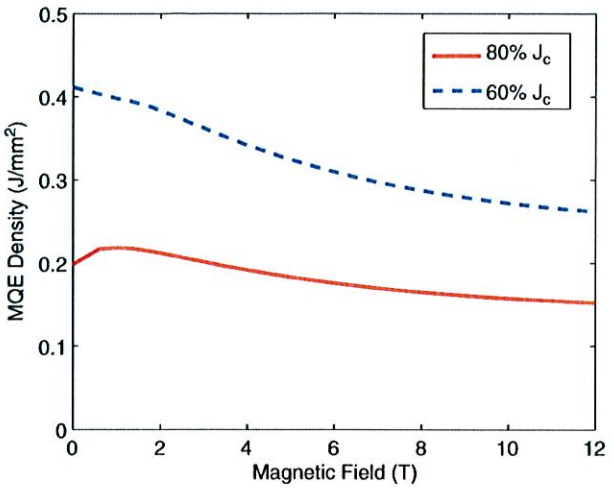

Fig. 3. Calculated minimum quench energy (MQE) as a function of applied magnetic field for current densities at 60% and 80% of J_c under adiabatic conditions.

the model and fit parameters that are given above. It is not clear how well the model predicts the entire critical surface since experimental data has not yet been obtained as a function of temperature.

V. Minimum Quench Energy and Normal Zone Propagation Velocity

In order to simulate an experiment where the minimum quench energy (MQE) and quench velocity are measured, a quench initiation heater is modeled by introducing heat into a region of length L_h for a duration t_h. This is done through the term Q_i in equation (8) where a non-zero value of Q_i is prescribed for $x_i < L_h/2$ over a duration t_h. The heat is only introduced over the region $x_i < L_h/2$ since only half of the domain is modeled due to symmetry. During the quench trigger, the temperature in the conductor will rise (possibly above the critical temperature), and once the quench trigger duration ends, the conductor can recover and dissipate the heat without an instability. However, if the temperature begins to rise again, then the instability is reached and a normal zone begins to propagate. Therefore, for the minimum quench energy calculation a quench is detected if $(\partial T/\partial t) > 0$ at the hot spot after a sufficiently long time has passed since the end of the quench trigger. This delay time is set to be $10t_h$, where this value was found to work well through trial and error. Fig. 3 shows the results from minimum quench energy calculation for current densities at 60% and 80% of J_c under adiabatic conditions. For this example, the heater duration time is set as $t_h = 50$ ms and the heater length is set at $L_h = 15$ mm. From Fig. 3 it is seen that the minimum quench energy decreases for applied magnetic fields from 2 T to 12 T at both 60% and 80% of J_c. Over this range there is a more rapid decrease in MQE for the case where the current density is chosen as 60% of J_c.

After the quench initiation, the normal zone will propagate away from the hot spot. The velocity at which this zone propagates is an important parameter for quench detection and magnet protection. In the simulations, the quench velocity is determined by finding the delay time over which two neighboring nodes become normal conducting. For example, the time at which a node at x becomes normal conducting is recorded. At a time Δt later the node at $x + \Delta x$ becomes normal conducting giving a normal zone propagation velocity of $\Delta x/\Delta t$ for that location at that time. The normal zone criterion is chosen to be such that a node is considered to be normal conducting when $J_2 = 0$ at that location. The normal zone propagation velocity is a time dependent quantity; however, a stable value is obtained after sufficient time has passed. The values reported here are the stable values that are obtained asymptotically. Fig. 4 shows the calculated normal zone propagation velocity as a function of applied magnetic field for current densities at 60% and 80% of J_c under adiabatic conditions. From this figure it is seen that the quench velocity drops at low fields but reaches a stable value in the applied magnetic field range between 3 T and 12 T. This initial drop in the normal zone propagation velocity is in agreement with the measurements reported in [5].

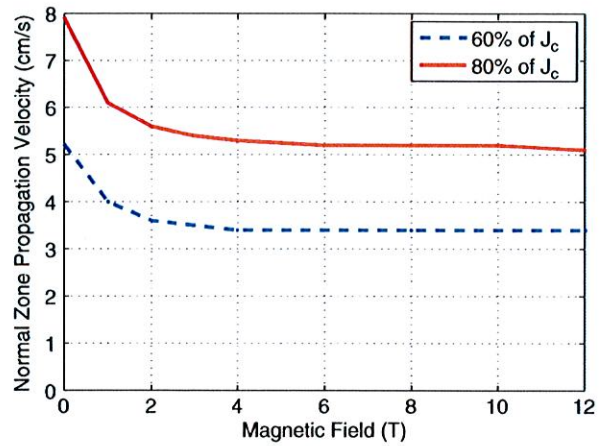

Fig. 4. Calculated normal zone propagation velocity as a function of applied magnetic field for current densities at 60% and 80% of J_c under adiabatic conditions.

In order to model the data that is obtained in a quench propagation experiment, simulated voltage taps are introduced at user specified locations in the numerical model. The temperature is also monitored at these locations as a function of time, since

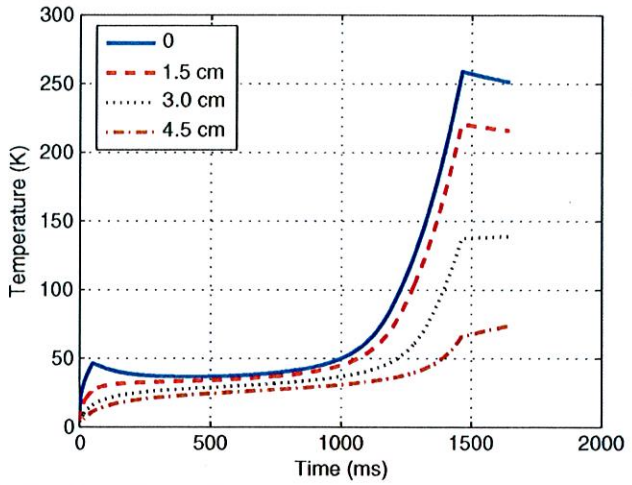

Fig. 5. Calculated temperature at the indicated locations for zero magnetic field and 80% of J_c under adiabatic conditions.

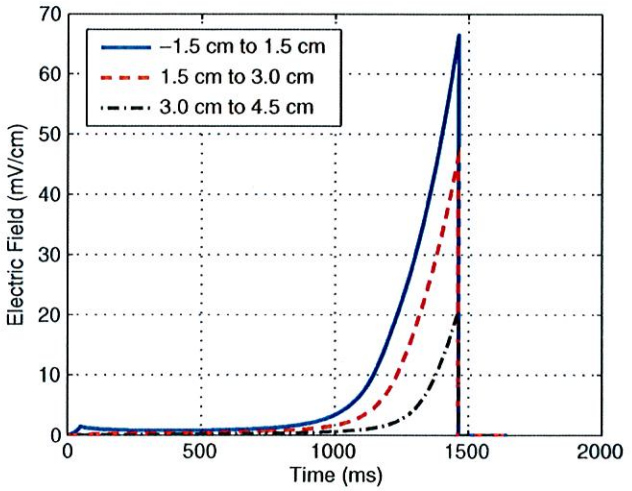

Fig. 6. Calculated electric field at the simulated voltage taps for zero magnetic field and 80% of J_c under adiabatic conditions. The electric field is obtained by dividing the calculated voltage by the distance between the voltage taps.

this is the type of information that can be obtained from an experiment. Fig. 5 shows the obtained temperature as a function of time at the hot spot (0) as well as 1.5 cm, 3.0 cm, and 4.5 cm away from the hot spot. For this simulation the following parameters were used: B = 0 T, the current density is taken at 80% of J_c, $t_h = 50$ ms, $L_h = 15$ mm, the heater power density is $Q_h = 5$ W/mm^2, where Q_h is defined as Q (see equation (1)) multiplied by the heater length. The temperature profiles show the initial rise in temperature due to the heat deposition through the heater. The hot spot temperature then begins to fall as the temperature redistributes away from this location. The conductor is in a state of current sharing at this point and eventually reaches an unstable point. At this point the hot spot temperature begins to rise again and the normal zone begins to propagate. The temperature then increases until a specified voltage criterion is met, at which point, the current is assumed to decay exponentially with a user specified time constant τ.

Fig. 6 shows the electric field between three different locations which are chosen as: −1.5 cm to 1.5 cm, 1.5 cm to 3.0 cm, 3.0 cm to 4.5 cm. In an experimental measurement this information would be used to determine the normal zone propagation velocity. This is done by setting a voltage criterion and determining the time duration during which the voltage at neighboring taps is equal to this criterion. As can be seen from Fig. 6, the voltage criterion must be chosen carefully in order to obtain meaningful results. For example, if the criterion is chosen too low the quench velocity value will be determined from the marginally stable zone (i.e. at a time below 1 s in the plot). This is not desirable since the quench has not yet begun to propagate at this point. If the voltage criterion is set too high the sample could also be damaged due to the high hot spot temperatures. For this example, an appropriate criterion could be chosen to be around 20 mV/cm. Note that with this criterion the quench propagation velocity is decreasing over the range of the two voltage taps. To reach a stable value, more voltage taps should be included away from the hot spot; however, the normal zone may not propagate very far in the amount of time necessary to avoid damaging the sample. Although a voltage criterion that is high enough is desired to accurately capture the normal zone propagation velocity, a lower voltage criterion is perhaps more desirable for quench protection. In this case the voltage criterion could be defined in the location of Fig. 6 where the voltage is steady and has not yet begun to rise rapidly (i.e. the current sharing regime).

VI. Conclusion

In this paper a one-dimensional numerical model for the analysis of the quench behavior of Bi2212 was presented. Understanding the quench behavior of these conductors is critical for their practical application in high field magnets. The work presented here focused on modeling of the quench behavior in an experimental setting where a single strand is used. Work has now begun in order to adapt this work to allow modeling of magnet quench protection. Another important issue associated with quench behavior is the degradation of the superconductor due to quenching. Work at LBNL is ongoing to develop dynamic models of thermal gradients and temperature induced strains in conductors. In [6], a multi-scale mechanical model of coils composed of Rutherford cables was presented. The coupling of the thermal quench propagation model with multi-scale mechanical models of strands and cables is an important step in understanding degradation due to thermal strains and gradients.

References

[1] A. Godeke, "Wind-and-react Bi-2212 coil development for accelerator magnets," *Superconductor Science and Technology*, vol. 23, no. 3, p. 034022, 2010.
[2] V. R. Romanovskii and K. Watanabe, "Multi-stable static states of Bi-based superconducting composites and current instabilities at various operating temperatures," *Physica C*, vol. 420, pp. 99–110, 2005.
[3] V. R. Romanovskii, "Current instability mechanisms in high-temperature superconductors cooled by liquid coolant," *Superconductor Science and Technology*, vol. 23, no. 2, p. 025020, 2010.
[4] L. Bottura, Note-CRYO/02/027 2002.
[5] L. Ye and J. Schwartz, private communication.
[6] D. Arbelaez *et al.*, "Cable deformation simulation and a hierarchical framework for Nb3Sn rutherford cables," *J. Phys.: Conf. Ser.*, vol. 234, p. 022002, 2010.